Published in final edited form as:
AIP Conf Proc. 2012 January 1; 1481: 381–387. doi:10.1063/1.4757365.

Overcoming Biological Barriers with Ultrasound

Dhaval Thakkar[a], **Roohi Gupta**[b], **Praveena Mohan**[b], **Kenneth Monson**[a], and **Natalya Rapoport**[b]

[a]Department of Mechanical Engineering, University of Utah, Salt Lake City, UT 84112, USA

[b]Department of Bioengineering, University of Utah, Salt Lake City, UT 84112, USA

Abstract

Effect of ultrasound on the permeability of blood vessels and cell membranes to macromolecules and nanodroplets was investigated using mouse carotid arteries and tumor cells. Model macromolecular drug, FITC-dextran with molecular weight of 70,000 Da was used in experiments with carotid arteries. The effect of unfocused 1-MHz ultrasound and and perfluoro-15-crown-5-ether nanodroplets stabilized with the poly(ethylene oxide)-co-poly(D,L-lactide) block copolymer shells was studied. In cell culture experiments, ovarian carcinoma cells and Doxorubicin (DOX) loaded poly(ethylene oxide)-co-polycaprolactone nanodroplets were used. The data showed that the application of ultrasound resulted in permeabilization of all biological barriers tested. Under the action of ultrasound, not only FITC-dextran but also nanodroplets effectively penetrated through the arterial wall; the effect of continuous wave ultrasound was stronger than that of pulsed ultrasound. In cell culture experiments, ultrasound triggered DOX penetration into cell nuclei, presumably due to releasing the drug from the carrier. Detailed mechanisms of the observed effects require further study.

Keywords

Cancer Therapy; Targeted Drug Delivery; Nanodroplets; Microbubbles; Perfluorocarbons; Ultrasound

INTRODUCTION

On the way to the intracellular target, drug has to overcome a series of biological barriers. We will discuss these barriers in relation to nanoparticle and ultrasound mediated tumor therapy. After the intravenous injection, the first barrier is formed by the endothelial lining of blood vessels. Tumor blood vessels are characterised by poorly organized vascular architecture and reduced lymphatic drainage; tumor vasculature is known to be much more permeable than blood vessels in normal tissues. Leaky blood vessels and the lack of a lymphatic system result in an increased interstitial fluid pressure, which hinders convectional transport of macromolecular drugs or nanoparticle drug carriers across blood vessel walls. Nevertheless, nanoparticles of appropriate size may accumulate in tumor tissue via the enhanced permeability and retention (EPR) effect based on defective tumor

PACS: 87.50.yt, 87.63.dh.

microvasculature. A characteristic pore cutoff size range between 380 and 780 nm has been shown in a variety of tumors although in some tumors the size may increase up to 2 μm. This allows extravasation of drug-loaded nanoparticles through large inter-endothelial gaps, while the poor lymphatic drainage of tumors results in longer retention of extravasated particles in tumor tissue.

After drug carrier penetrates through the vessel wall into tumor tissue, cell plasma membranes create the next barrier. For most drugs, site of action is located in the interior of the cells, i.e. in the cytoplasm or nucleus. To be effective, drug has to overcome the plasma membrane barrier and often some intracellular membranes as well. For instance, if internalized by endocytosis, drug or gene is localized in endosomes or lysosomes and have to get out of these organelles to be effective. Moreover if the site of action is in the nucleus (as for instance for anthracyclin drugs), drug has to overcome the nuclear membrane to realise its chemotherapeutic potential.

In addition, tumors are usually heterogenous matrices with some components of tumor tissue creating physical barriers for drug carrier and drug diffusion throughout tumor tissue which creates drug gradients that may be responsible for inducing drug resistance.

These issues impair the activity of anticancer drugs. In what follows, we show in model experiments using excised blood vessels and cell cultures that local application of therapeutic ultrasound helps in overcoming sequential biological barriers.

MATERIALS AND METHODS

Block copolymers

Block copolymers used in this study were bought from Polymer Source (Quebec, Canada). The poly(ethylene oxide)-co-poly(D,L-lactide) (PEG-PDLA) copolymer had a total molecular weight of 9,500. The poly(ethylene oxide)-co-polycaprolactone (PEG-PCL) copolymer had a total molecular weight of 4,600 D.

Micellar solutions and drug loading

Micellar solutions of the block copolymers were prepared by a solvent exchange technique as described in detail previously [1–4]; doxorubicin (DOX) or paclitaxel (PTX) loading into the micelles was performed at the nanodroplet preparation stage.

Preparation of nanoemulsions

An aliquot of perfluorocaarbon (perfluoro-15-crown-5-ether, PFCE) or perfluoropentane (PFP) was pipetted into a corresponding micellar solution and sonicated by 20-kHz ultrasound in ice-cold water for emulsification.

Nanoparticle size distribution

Size distribution of nanoparticles was measured by dynamic light scattering at an angle of 165° using Delsa Nano S instrument (Beckman Coulter, Osaka, Japan) equipped with a 658

nm laser and a temperature controller. Size distribution was analyzed using Non-Negative Least Squares (NNLS) method.

Cell culture

A2780 ovarian cancer cells were cultured in RPMI-1640 medium (Sigma Aldrich, St Louis, MO) supplemented with 10% heat deactivated fetal bovine serum (FBS) (USA Scientific Inc., Orlando, FL) and 1% penicillin–streptomycin (Sigma Aldrich, St Louis, MO). The cells were maintained at 37 °C in a humidified atmosphere with 5 % CO_2.

Sonication

Unfocused 1-MHz ultrasound was generated by an Omnisound 3000 instrument (Accelerated Care Plus Inc, Sparks, NV) equipped with a 5 cm^2 transducer head. Ultrasound pressure was measured using Onda needle hydrophone (Onda HNR-0500) placed in front of the probe with a distance of 0.5 cm from the probe.

Cells were grown either on cover slips in special 35 mm glass bottom cutlure dishes (Mattek Corporation, Ashland, MA) or in 10-mL capacity OptiCell units (Biocrystal, Westerville, OH) to 90% confluence. Prior to sonication, growth medium was removed and the glass bottom chamber or OptiCell was completely filled with a desired formulation; cells were incubated in the formulation for 20 minutes at 37 °C before sonication. Ultrasound direction was from the top of the chamber towards the cell-coated bottom in order to prevent cell detachment. After ultrasound treatments, cells were imaged with confocal microscope (Olympus IX81, Olympus America Inc., Center Valley, PA). Emission filters were 570 nm for DOX and 480 nm for Hoechst or DAPI (if used). Image slices of the cells were recorded at an incremental step of 0.5 μm from the bottom to the top of the cell layer in the z-direction. The images recorded were stacked in the z-direction and processed using ImageJ software. For each formulation, the chamber or the OptiCell unit with sham sonication was used as a control.

Sonication of excised carotid arteries

Carotid arteries were excised from Swiss Webster white mice obtained from Charles River Laboratories (Wilmington, MA). Animals were housed in accordance with the Guide for the Care and Use of Laboratory Animals as adopted by the National Institutes of Health. Freshly excised arteries were mounted between two siringe needles and installed in the experimental setup described below.

Experimental setup for studying the effect of ultrasound on the carotid artery permeability consisted of acrylic bar fixtures designed to hold the needles, plastic cuvette with a PBS solution through which a lower needle passed, and water bath to immerse the ultrasound probe. Blood vessel ends were tied to blunt-tipped, luer-hub, 30 G needles using 6-0 silk suture. Figure 1 shows the schematic diagram of the experimental setup.

The permeability of carotid arteries was measured for FITC-dextran of 70,000 Da molecular weight. In permeability tests, 0.05% lysine fixable FITC-dextran solution mixed or not mixed with 1% PFCE/5% PEG-PDLA nanodroplets was gently injected into the blood

vessel from the lower needle, upon which the blood vessel was exposed to ultrasound. Unfocused 1-MHz ultrasound was applied at a nominal power density of 3.0 W/cm^2; due to proximity of the transducer to the blood vessel (about 7 mm), sonication proceeded in the ultrasound near field. Continuous wave (CW) ultrasound was applied for 1 min; pulsed ultrasound with a 33% duty cycle was applied for 3 min, which produced equal ultrasound exposure time for both CW and pulsed ultrasound. Temperature measurements with needle thermocouple positioned next to the sham vessel during sonication showed that the ultrasound-induced temperature increase was very marginal; maximum temperature never rose to or above 37 °C.

The total time of artery incubation with the formulation was 10 minutes independent of, if ultrasound was applied or not during the incubation period. After 10 minutes of incubation, FITC-dextran formulation inside the vessel was replaced with a 4% paraformaldehyde solution for artery fixation. Blood vessel was then taken out of the set and inserted into the bath with a 4% paraformaldehyde where it was kept until being inserted into the paraffin block and sliced into 200 μm slices for confocal imaging.

RESULTS AND DISCUSSION

Ultrasound and nanodroplet effect on the FITC-dextran penetration through the carotid artery wall (research in progress)

Six experimental groups were used in these experiments:

1. control (FITC-dextran, no droplets, no ultrasound)
2. FITC-dextran, droplets, no ultrasound
3. FITC-dextran, no droplets, CW ultrasound
4. FITC-dextran, droplets, CW ultrasound
5. FITC-dextran, droplets, pulsed ultrasound
6. CW Ultrasound applied 3 min before the injection of FITC-dextran and nanodroplets.

Two or sometimes three repetitions were performed within each group. Representative confocal images of arterial slices are shown in Figure 2. Without nanodroplets, very marginal (if any) effect of ultrasound on the FITC-dextran penetration through the arterial wall was observed (data not shown). Likewise, no effect of droplets on the FITC-dextran penetration was observed without ultrasound (Figure 2, left). The application of ultrasound with nanodroplets noticeably enhanced FITC-dextran penetration through the arterial wall (green color); with the same exposure time and energy, the effect of CW ultrasound was much stronger than that of pulsed ultrasound (Figure 2, compare the central and right panels). Moreover, with the application of ultrasound, penetration of droplets through the arterial wall was clearly seen at higher magnification. Interestingly, PFCE/PEG-PDLA nanodroplets acquired fluorescence in interaction with FITC-dextran, which allowed their demarcation in fluorescence images of arterial slices.

The effect of CW ultrasound was clearly very directional (Figure 2). In one sample, separation of the intimae and adventitia from the arterial wall was observed.

The data obtained presented show that (1) penetration of macromolecules and nanoparticles through blood vessel walls is enhanced by ultrasound; (2) at the same delivered total energy, the effect of CW ultrasound is much stronger than that of pulsed ultrasound; (3) the effect of ultrasound is directional. The differences between the effects of pulsed and CW ultrasound may be, at least partly, attributed to the thermal effect that was much more pronounced for CW that for pulsed ultrasound though final temperature under ultrasound never reached physiological range.

The data presented above imply that the radiation force plays an important role in enhancing macromolecule and especially nanodroplet penetration through arterial walls, as was shown earlier for microbubbles by Ferarra's group [5–7]. We have observed that PFCE nanodroplets convert into microbubbles under the action of ultrasound []. Microbubble "pushing" against the vessel wall and oscillations in the close vicinity to a vessel wall may be responsible for the additional opening of the inter-endothelial gaps, which enhances vessel permeability. This effect has been used for opening of the blood brain barrier in works by Hynynen and McDannold's groups [8,9].

Overcoming cellular membrane barriers with ultrasound

The results presented below show that oscillation and cavitation of the bubbles formed under ultrasound from perfluorocarbon nanodroplets triggers the release of the nanodroplet encapsulated drug from the carrier as well as perturbs cell membranes thus enhancing the intracellular uptake of both, nanodroplets and drugs. In the present study, fluorescence was imparted to PFCE/PEG-PCL emulsions by introduction of a fluorescent phospholipid 1,2-distearoyl-sn-glycero-3-phosphoethanolamine-N-carboxyfluorescein [(polyethylene glycol)-2000] (ammonium salt) (Avanti Polar Lipids, Alabaster, AL) into droplet shells. Ovarian carcinoma A2780 cells were incubated with the fluorescent formulations. The laser confocal images of cells indicated that nanodroplets were internalized by tumor cells but did not penetrate into cell nuclei (Figure 3); application of ultrasound did not change nanodroplet extranuclear localization.

In the other set of experiments, nanodroplet fluorescence was imparted by a fluorescent drug (Doxorubicin, DOX) encapsulated in nanodroplet shells. Intracellular distribution of Doxorubicin was monitored with and without ultrasound []. The data showed that without ultrasound, DOX was localized in the extracellular space, presumably being internalized within nanodroplets; after the application of ultrasound, DOX was found in cell nuclei where its site of action is localized (Figure 4); this effect was most probably caused by DOX release from the nanodroplet carrier [10].

Summarizing, application of therapeutic ultrasound enhanced macromolecule and nanodroplet penetration through all biological barriers probed in this study.

Acknowledgments

This work was supported by the NIH grant R01 EB1033 of N.R.

REFERENCES

1. Rapoport N, Gao Z, Kennedy AM. J. Natl. Cancer Inst. 2007; 99:1095–1106. [PubMed: 17623798]
2. Rapoport N, Nam K-H, Gupta R, et al. J. Control Release. 2011
3. Rapoport NY, Efros AL, Christensen DA, et al. Bub Sci Eng Tech. 2009; 1(1–2):31–39.
4. Rapoport NY, Kennedy AM, Shea JM, et al. J Control Release. 2009; 138(3):268–276. [PubMed: 19477208]
5. Dayton P, Klibanov A, Brandenburger G, et al. Ultrasound Med Biol. 1999; 25(8):1195–1201. [PubMed: 10576262]
6. Dayton PA, Zhao S, Bloch SH, et al. Mol Imaging. 2006; 5(3):160–174. [PubMed: 16954031]
7. Ferrara KW. Advanced drug delivery reviews. 2008; 60(10):1097–1102. [PubMed: 18479775]
8. Hynynen K. Advanced drug delivery reviews. 2008; 60(10):1209–1217. [PubMed: 18486271]
9. McDannold N, Vykhodtseva N, Hynynen K. Ultrasound Med Biol. 2008; 34(6):930–937. [PubMed: 18294757]
10. Mohan P, Rapoport N. Molec. Pharmaceutics. 2010; 7(6):1959–1973.

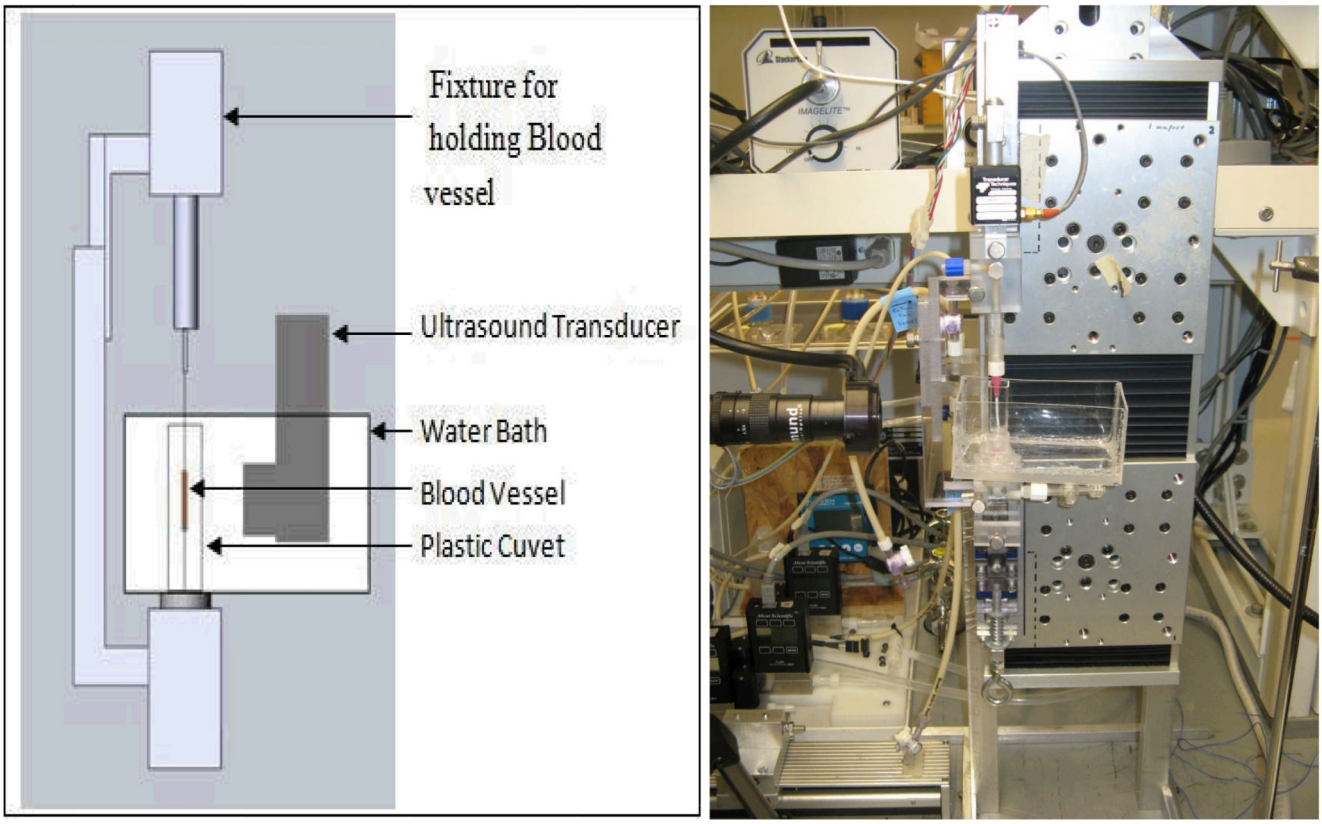

Figure 1.
Schematic representation (left) and a photograph (right) of the experimental setup in the experiments on the ultrasound-modulated permeability of the carotid arteris. In the photograph on the right, the artery is replaced with a thin plastic tube.

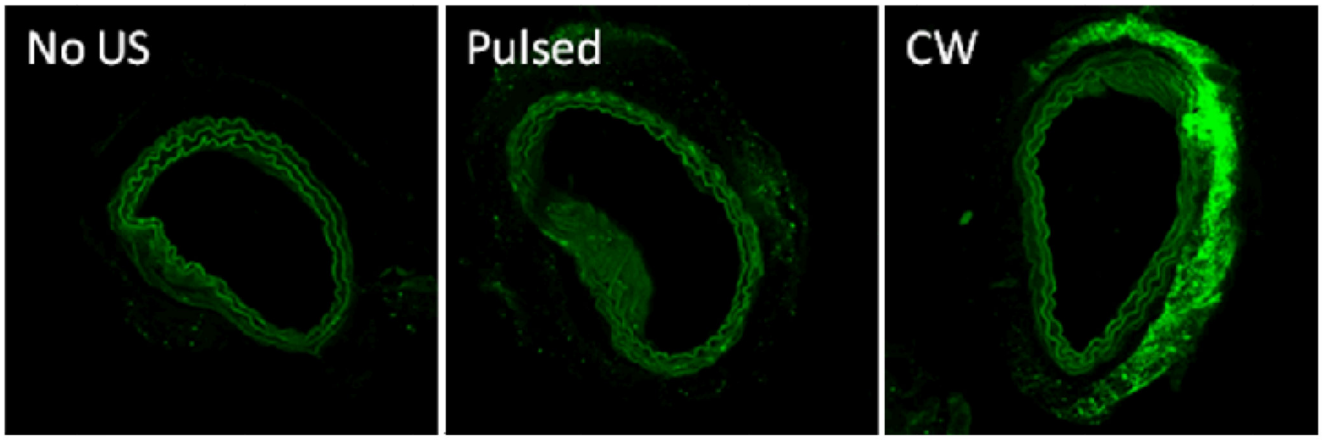

Figure 2.
Fluorescence images of arterial slices for arteries incubated or sonicated in the presence of nanodroplets: left - without ultrasound, center – pulsed ultrasound, right – CW ultrasound.

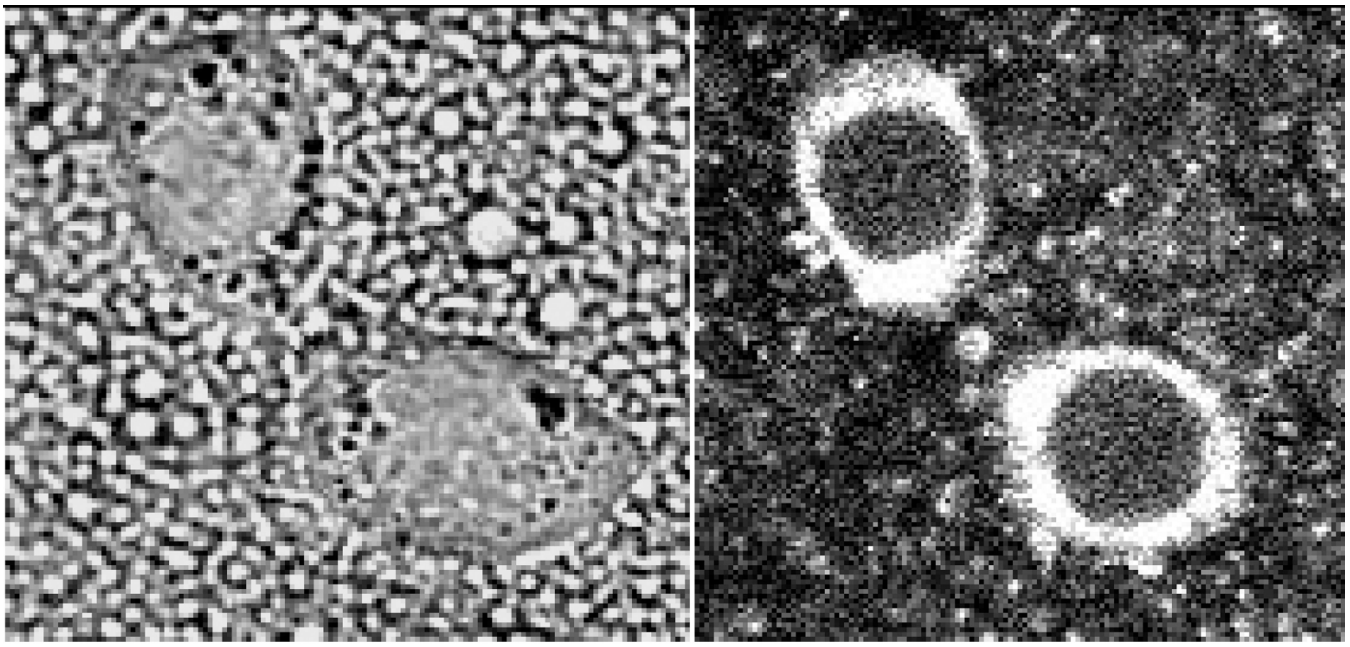

Figure 3.
Fluorescently labeled PFCE/PEG-PCL nanodroplets wre internalized by A2780 cells but did not penetrate into cell nuclei even under the action of 1-MHz, 3.4 W/cm^2 power density ultrasound delivered for 1 min.

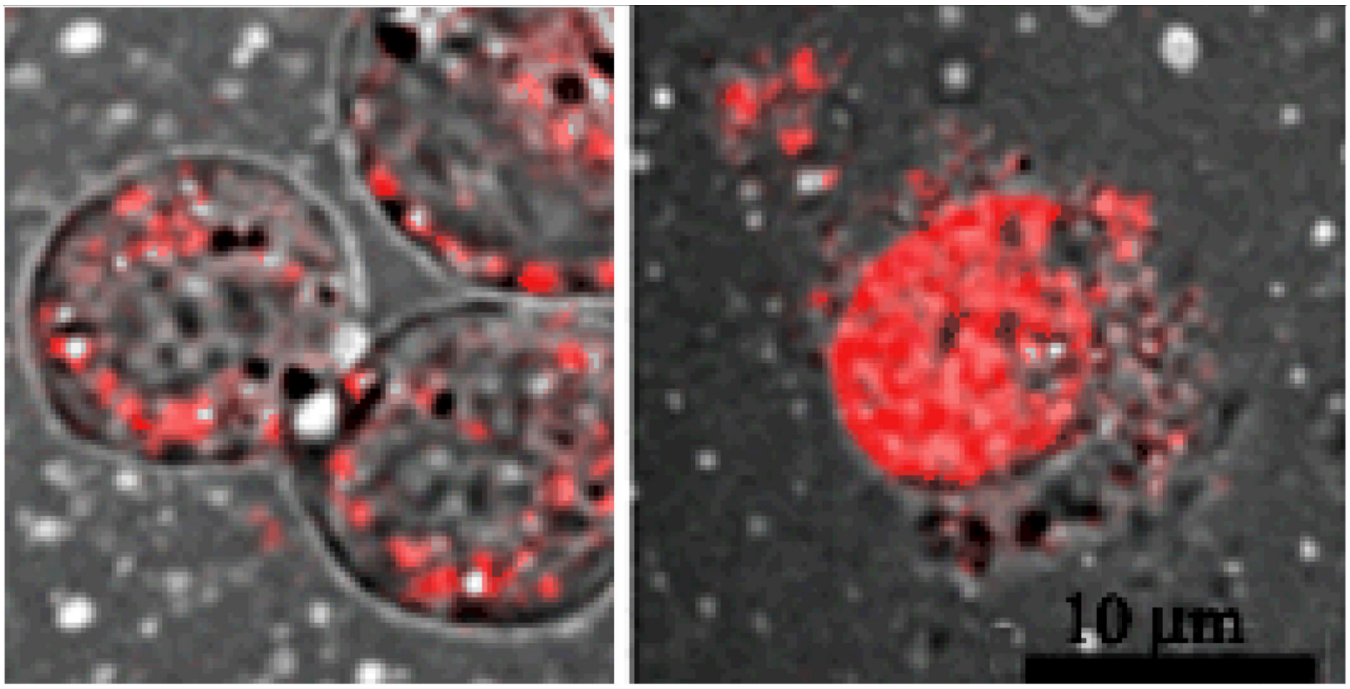

Figure 4.
DOX delivered inside PFCE/PEG-PCL nanodroplets did not penetrate into cell nuclei without ultrasound but was localized in cell nuclei after the application of ultrasound.